Medical Engineering & Physics 34 (2012) 1149–1156

Contents lists available at SciVerse ScienceDirect

Medical Engineering & Physics

journal homepage: www.elsevier.com/locate/medengphy

Influences of supra-physiological temperatures on microstructure and mechanical properties of skin tissue

Min Lin[a,b,1], Xiao Zhai[b,1], Shuqi Wang[c], Zhengjin Wang[b], Feng Xu[a,b,c,*], Tian Jian Lu[b,**]

[a] The Key Laboratory of Biomedical Information Engineering of Ministry of Education, School of Life Science and Technology, Xi'an Jiaotong University, Xi'an 710049, PR China
[b] Biomedical Engineering and Biomechanics Center, Xi'an Jiaotong University, Xi'an 710049, PR China
[c] HST-Center for Biomedical Engineering, Department of Medicine, Brigham and Women's Hospital, Harvard Medical School, Boston, MA, USA

ARTICLE INFO

Article history:
Received 18 December 2010
Received in revised form
29 November 2011
Accepted 2 December 2011

Keywords:
Thermal damage
Microstructure
Skin tissue
Mechanical behavior
Arrhenius burn integration

ABSTRACT

Thermal therapies under supra-physiological temperatures are increasingly used to treat skin diseases (*e.g.*, superficial melanoma, removal of port-wine stains pigmented and cutaneous lesions). The efficacy of these therapies depends on the thermal and mechanical loadings that skin experiences during the treatment process. Therefore, it is of great significance to better understand the role of thermally induced changes in skin mechanical behavior and microstructure. In this study, rabbit belly skin was thermally damaged by immersing skin samples into saline solutions with controlled temperatures. We investigated the effect of thermal damage on skin mechanical behavior. We quantified the changes in skin microstructure (*i.e.*, fiber, fibril) using histological staining and transmission electron microscopy (TEM). The results indicate that (i) the elastic modulus of skin, obtained by the uniaxial tensile test, decreased with increasing heating temperature; (ii) the skin tensile behavior was correlated with its microstructure changes induced by thermal denaturation of collagen fibers under supra-physiological temperatures; (iii) skin thermal damage predicted using the Arrhenius burn integration quantitatively agrees well with the evolution of the microstructure (*i.e.*, percentage of the collagen area in Hematoxylin and Eosin (H&E) staining results). This study provides a better understanding of the coupled bio-thermo-mechanical behavior of skin tissue that could help to improve clinical thermal therapies.

1. Introduction

Thermal therapies under supra-physiological temperatures (*e.g.*, via laser and microwave) find widespread applications in clinical treatment of skin diseases, such as the removal of port-wine stains [1,2], pigmented and cutaneous lesions [3,4]. For hyperthermia of superficial melanoma, the skin tissue is heated to a temperature above a critical value (~43 °C) [5]. During this process, there is significant change in the mechanical properties and structure of the skin and the skin thermal damage occurs [6]. Besides, skin tissue may be under both thermal and mechanical loadings during these therapies. For instance, epidermal pigmented lesions are treated with the compression technique under laser irradiation [7]. Therefore, the success of these therapies requires precise control over the thermal and mechanical loadings that skin experiences [6], which requires the better understanding on the changes in skin mechanical properties and structure at supra-physiological temperatures.

The mechanical behavior of biological tissues (*e.g.*, skin) has a close relationship with their microstructure [8]. Most natural tissues have a hierarchical structure and are composed of composite materials made from fibers to support mechanical loads [9,10]. Collagen, which has a triple-helix structure, is a component of various hard tissues (*e.g.*, bone, tooth enamel and shell) and primary element of soft tissues (*e.g.*, skin, tendon and cartilage). Although these collagenous tissues are composed of fibers with similar structures, their mechanical behaviors vary significantly which depend on the assembly methods of the fibers. For example, the elastic modulus of collagen fibers is around 1–1.5 GPa [11], while those of cortical bone and human skin are 8–24 GPa [11] and 0.42–0.85 MPa [12], respectively.

Skin dermis has a large number of collagen fibers and is considered to be a major force-bearing component. Supra-physiological temperature can induce thermal denaturation of skin collagen, which is observed as thermal shrinkage of collagen at microscale. The collagen irreversibly changes from a native helical structure to a random structure after thermal damage [13]. The thermally induced breaking of hydrogen bonds within college leads to the

* Corresponding author at: Biomedical Engineering and Biomechanics Center, Xi'an Jiaotong University, Xi'an 710049, PR China.
** Corresponding author.
E-mail addresses: fengxu@mail.xjtu.edu.cn (F. Xu), tjlu@mail.xjtu.edu.cn, minlin0591@gmail.com (T.J. Lu).
[1] These authors contributed equally.

1350-4533/$ – see front matter © 2011 IPEM. Published by Elsevier Ltd. All rights reserved.
doi:10.1016/j.medengphy.2011.12.003

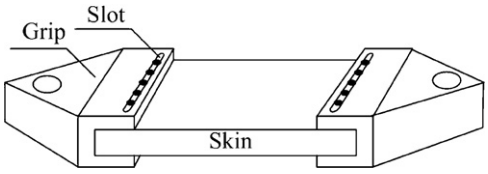

Fig. 1. Schematic of uniaxial tension test.

changes of skin mechanical properties at macroscale [14]. Previous studies have shown that thermal damage has an effect on skin mechanical behavior [15–20] through regulating two heating parameters, *i.e.*, temperature level and duration of heating [21–23]. When thermal damage occurs, the intramolecular cross-links in dermal collagen will break, inducing changes in mechanical behavior (*e.g.*, decreased elastic modulus) [24]. However, there are limited studies on the quantitative relationship between collagen fiber structure under supra-physiological temperatures and mechanical loading.

To address this issue, we studied the mechanical behavior of thermally damaged skin tissue under uniaxial tension, examined the corresponding changes of skin microstructure (*i.e.*, fiber and fibril), and quantified the thermal damage of collagen fibers using histology analysis. We compared the experimental results with mathematical predictions using Arrhenius burn integration proposed by Henriques and Moritz [25,26].

2. Materials and methods

2.1. Specimen preparation

Five male rabbits with a body weight of 1.5 kg were provided by the Animal Center of Xi'an Jiaotong University. Before sampling, the hair on the rabbit skin was removed using an electrical hair clipper. Skin samples were procured from the belly immediately after sacrifice. Rectangular specimens ($50 \times 6 \times 0.6\,mm^3$) were cut from the excised skin samples, with the direction of long axis parallel to the backbone of the rabbit. The *in vitro* dimensions was measured since they were smaller than the *in vivo* case due to the contraction of skin tissue after excision. The rectangular specimens were then stored at 4 °C in saline solution according to standard tissue procurement protocol. To minimize the degradation of the tissue, the tests were completed within a few hours. The experimental protocol was approved by the Animal Care and Use Committee of the University.

2.2. Thermal damage tests

Thermal damage tests were performed without applying any mechanical loading. There were five specimen groups for the thermal damage test and the specimens in the same group were from the same rabbit (prior to the experiment, the skin from different rabbits were tested at room temperature, the mechanical behavior were similar). The five groups of skin specimens were immerged into saline solutions in measurement chambers heated to a constant temperature of 37 °C, 45 °C, 50 °C, 60 °C or 70 °C, respectively, for 10 min. To achieve uniform solution temperature, the chamber was thermally insulated and the solution was stirred. After heating, the specimens were quenched in room temperature solution (25 °C) for 60 min and then kept in 10% neutral buffered formalin for two days until histology test. The specimens heated at 37 °C were used as the control.

2.3. Uniaxial tension tests

A self-designed thermo-mechanical testing system which has been calibrated in our previous work [20,27] was used to exert a variety of repeatable mechanical loading on specimens. The system consists of a computer-controlled step motor (hybrid 1.8°), a screw system, load cells, loading carriages. The specimens described in Section 2.2 were mounted in the system using two grips with their axis parallel to the tensile loading. Since it is challenging to

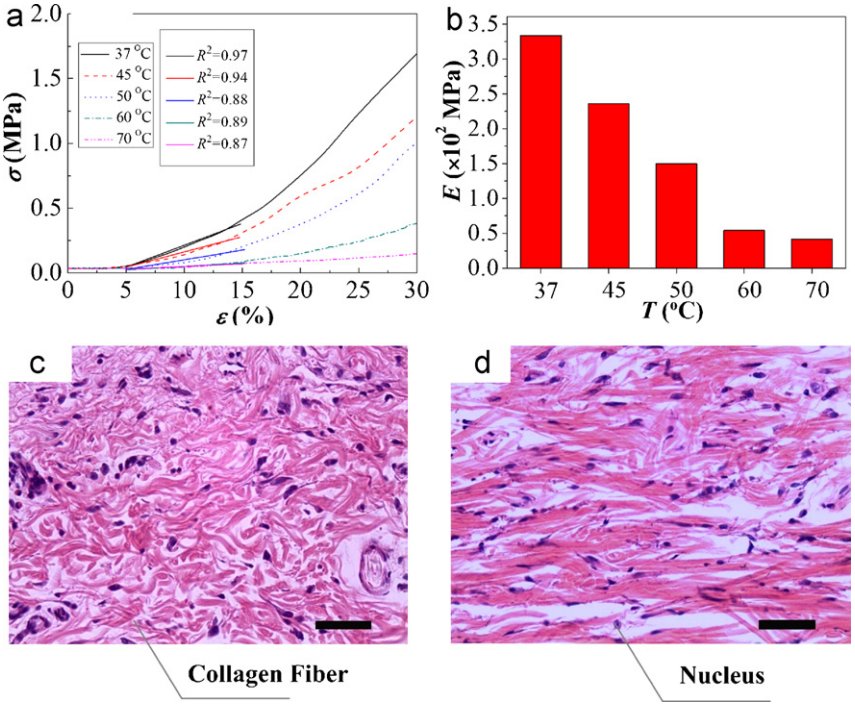

Fig. 2. Thermal damage induced change in mechanical behavior of the skin. (a) The stress–strain relationship under uniaxial tensile loading; (b) changes in modulus after thermal treatment under different temperatures; the changes of microstructures of skin before (c) and after (d) stretch in saline solution at 37 °C are also shown. The direction of force in (c) is horizontal. Scale bar: 10 μm.

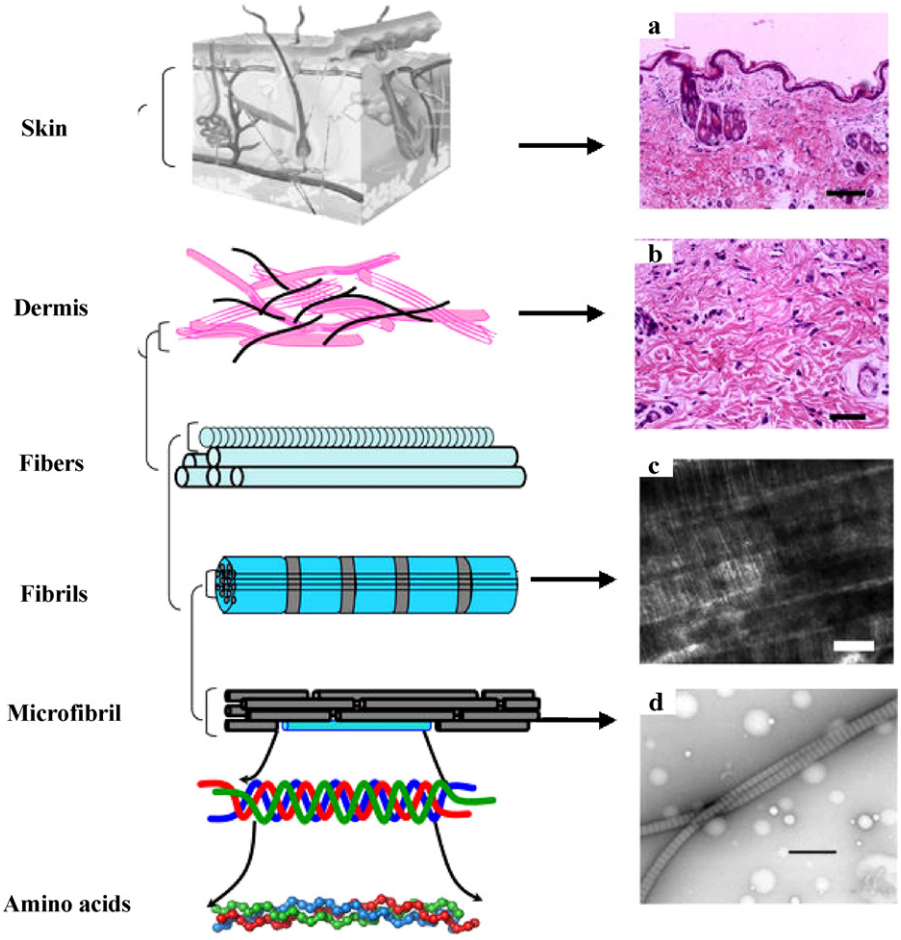

Fig. 3. Multi-scale structure of skin tissue. On the left is the length scale for relative components. In the middle column are the sketch maps of collagen and in the right column are the pictures obtained from experiments. Scale bar: 40 μm in (a), 5 μm in (b), 100 nm in (c) and 500 nm in (d) [43]. The sketch map of skin is adapted from Ref. [33].

connect the tissue to the load cell, we have designed special grips with a 0.12 mm wide, 18 mm long slot (Fig. 1). The skin sample was fixed in the grip using five pins with diameter of ~0.1 mm through the slot. In this way, the sample can expand freely in the lateral direction during tensile test. The grips were connected to the load cells. The specimen was stretched at a rate of 0.2 mm s^{-1}. The original length of the specimen served as the reference point for all the subsequent measurements. The force was stopped when the length of the stretched specimen reached up to 1.3 times of the original length (*i.e.*, a engineering strain of 30%). To accurately observe the effect of tensile force on the arrangement of collagen fibers (*i.e.*, fiber alignment), each of the tested specimen was nailed on a board at the end of tensile testing (before removed from testing machine) for maintaining their stretched length. The specimens and the boards were removed from the testing machine and were then kept in 10% neutral buffered formalin for two days to prevent retraction.

Tensile force was measured using load cells and then processed using an integrated software system developed in LabView. The stress (*i.e.*, engineering stress) was obtained by dividing the tensile force with the initial cross-section area of the specimens. Nine markers were made on the specimen surface using a surgical marker pen. To minimize the effect of local stress concentrations of the gripping attachments, the strains were measured from central region of the specimens. Through tracking the markers on the surface of the specimen, in-plane finite strains and deformations in the tissue were measured optically with a CCD camera. The strains were obtained by comparing current marker positions (*e.g.*, pixel coordinates) to the reference positions. The accuracy of the strains relies on high-resolution, high-sampling rate of the video.

2.4. Histology analysis

H&E staining was used to analyze skin histology. The specimens from thermal damage tests (specimens at room temperature and those heated at different temperatures) and uniaxial tension tests (specimens before and after mechanical loading, separately) were embedded in paraffin blocks and subsequently subjected to microscopic sections (~5 μm in thickness, 5 different sections per sample and 10 images per section). The part in the center of specimen, was cut along tensile direction and stained with H&E staining. Histological images were captured using light microscope and analyzed with the NIH free software ImageJ. The area of melted collagen fibers was quantified according to the pixels intensity using the image data from the histological results.

2.5. TEM observation

Transmission electron microscopy (TEM) was used to analyze the structural changes induced by thermal damage at ultrastrutural level. The specimens were immerged into the saline solution at 60 °C for 30 s, fixed in 2% (v/v) glutaraldehyde for 2 h at 4 °C, and then fixed with 1% (w/v) osmium tetroxide for 2 h after being rinsed several times with phosphate buffer (PBS, pH 7.4). The specimens

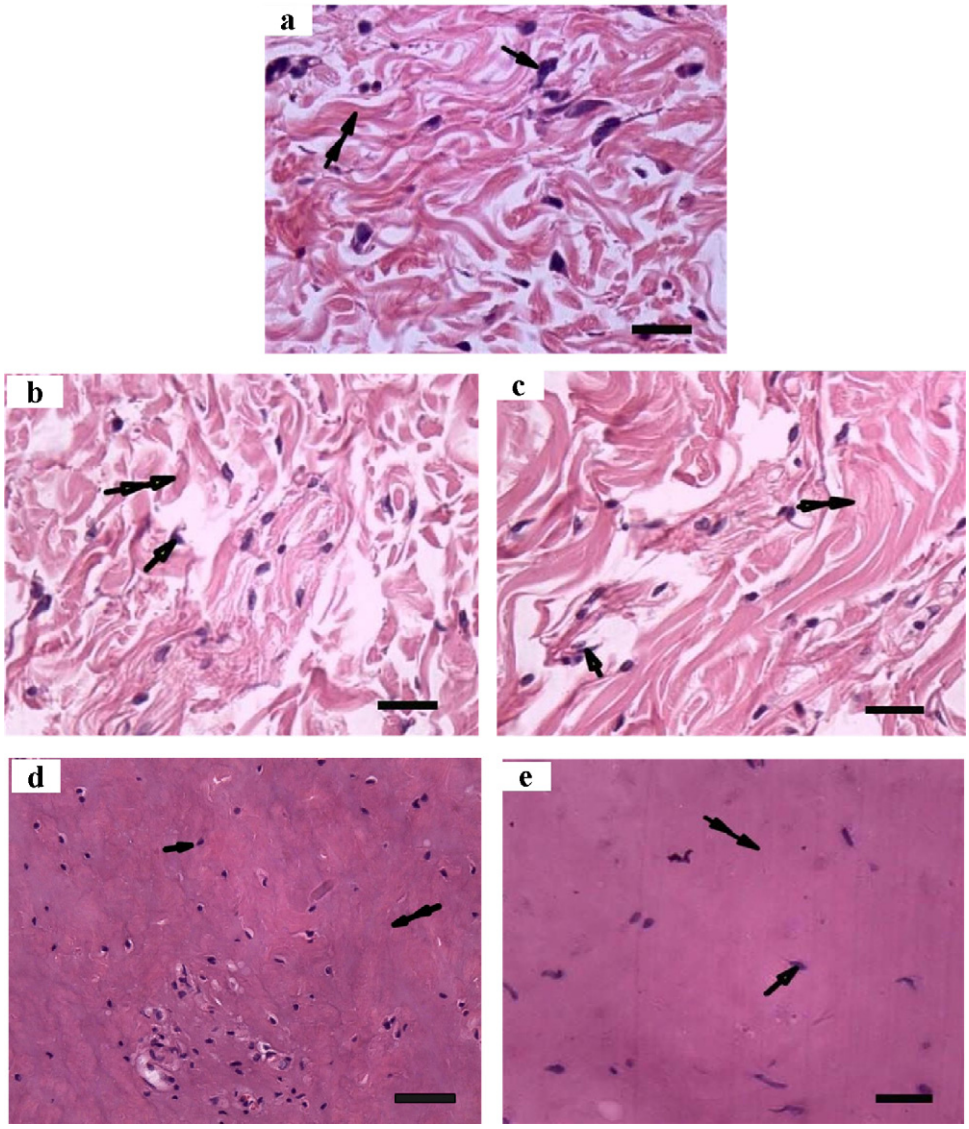

Fig. 4. Thermal damage induced changes in skin microstructure. (a)–(e) show the H&E staining results of rabbit belly skin after heating in the saline at 37 °C (a), 45 °C (b), 50 °C (c), 60 °C (d) and 70 °C (e) for 10 min, respectively. The regions denoted by the double and single arrowheads represent collagen fibers and cell nuclei. Scale bar: 5 μm.

were dehydrated and embedded in Epon 812. Ultrathin sections (60 nm) were stained using uranyl acetate. The TEM results of the thermally damaged samples were compared with those of the control samples (heated at 37 °C) to investigate the microstructure changes induced by thermal damage.

3. Results and discussion

3.1. Influence of thermal damage on skin mechanical behavior

To check the influence of thermal damage on the skin mechanical behavior, we tested the uniaxial tensile behavior of skin samples thermally damaged under different temperatures (Fig. 2a). We observed that the trends of mechanical characteristics for the damaged specimens are similar to those of the controls. That is, they all display a non-linear load response, which is in accordance with our previous findings [28]. The stress–strain curve dominated by collagen fibers can be divided into three parts [29]. In the low stress part, called the 'toe region', the curve is almost horizontal. Under low stress, elastin fiber, highly flexible, is first stretched [29,30] and large numbers of collagen fibers are presumably crimped; therefore, response at the low level of stain involves little collagen fiber stretching. The second part, called 'heel region', is nonlinear, and the majority of the fibers in skin are gradually stretched. The third part is the 'linear region', where all the fibers are sufficiently stretched along the direction of the force [31].

Thermal damage induced changes in skin mechanical behavior could also be identified from changes in modulus. We quantified the modulus (linear fit of stress–strain curves in Fig. 2a with strains range between 5% and 15%) after thermal treatment under different temperatures, Fig. 2b. We observed significant decrease in modulus for skin specimens after thermal treatment with saline solution at 45 °C, 50 °C, and 60 °C, respectively. As compared with that of 60 °C, slight decrease in modulus upon thermal treatment with 70 °C saline solution indicates that severe thermal damage occurs when temperature rises above 60 °C.

It can be observed from Fig. 2a that the skin got stiffer with increasing strain, especially at 37 °C, 45 °C, and 50 °C. To verify the role of collagen fibers, we analyzed their distribution before (Fig. 2c) and after (Fig. 2d) the skin specimens were stretched in the saline solution at 37 °C (without thermal damage). The tensile direction is shown by the staining results (horizontal in Fig. 2c and d). We

observed that the collagen fibers changed from a random pattern in the original tissue to the alignment in parallel with the loading direction in the stretched tissue. It is generally accepted that the changes in the direction of collagen fibers can strengthen the skin mechanical behavior [32]. The specimens heated at temperatures of 45 °C and 50 °C showed similar changes in collagen fiber alignment as those heated at 37 °C (data not shown here for brevity). As in the cases of 60 °C and 70 °C, most of the collagen fibers were melted (see details in the following section). Hence the collagen fibers alignment could hardly be identified.

The stress–strain curves of rabbit skin with different thermal damages (*i.e.*, heated for 10 min at 37 °C, 45 °C, 50 °C, 60 °C and 70 °C, respectively) show that skin stiffness decreased with increasing temperatures, primarily due to the change in the structure of collagen fibers [32]. The multi-scale structure of skin was introduced to explain the macro mechanical behavior of skin tissue. In the middle column of Fig. 3 are the sketch maps of collagen and in the right are the pictures obtained from experiments. The selected praline and lysine (both are a kind of α-amino acid) are hydroxylated and glycosylated. Three pro-α chains, assembled around each other by van der waals force and covalent bond, form a triple helix structure (*i.e.*, the collagen molecule). The collagen molecules, approximately 300 nm in length and 1 nm in diameter, attach to the adjacent molecules, forming fibrils with a diameter of 50 nm by intra-fibrilar bonding. Fibrils display a characteristic periodicity of 67 nm, which can be recognized by electron microscopy and atomic force microscopy [33]. The collagen fibril, therefore, plays a critical role in scaffolding structures from the nanoscopic scale to macroscopic scale [33]. The collagen fiber is composed of the collagen fibrils, which are organized into more complex patterns and form three dimensional networks in the skin dermis [6].

Thermal damage induced change in extensibility (Fig. 2a) can be explained by theory of composite materials [34]. Collagen fibers are the main component in skin tissue that is responsible for the resistance to tensile loading. When the collagen fibers are thermally damaged, the resistance to tensile loading reduced and the skin tissue exhibits increased extensibility. On the other hand, there is a small amount of glycosaminoglucan (GAG) exists in skin matrix, which interacts with fibers providing resistance to the sliding of collagen fibers [35]. Supra-physiological temperature alters the properties of GAG and reduces its content leading to the easy sliding of fibers [35]. It was assumed that elastin fibers may play a more influential role than collagen fibers in the tissue extensibility due to their thermal stability and rubber-like mechanical behavior [36].

3.2. Influence of temperature on collagen fiber structure

The changes in collagen structure at various macromolecular levels (*e.g.* histological analysis, TEM) were investigated to better understand the mechanism behind denaturation. When skin temperature rises above a critical value (~43 °C), denaturation occurs [25]. To investigate the influence of heating time and temperature on the structure of collagen fiber, we checked the skin structure using histology method (H&E staining) for rabbit belly skin heated at 37 °C, 45 °C, 50 °C, 60 °C and 70 °C for 10 min, Fig. 4a–e. The regions denoted by the double and single arrowheads represent collagen fibers and cell nucleus, respectively. The blank domain among collagen fibers was the tissue fluid in natural tissue. As described above, the component unit of the fiber is collagen molecule with a triple helix structure and such collagen molecules help strengthen skin tissue [37]. The intramolecular cross-links of collagen were ultimately broken with heating (as shown in Fig. 5). The collagen transformed from a highly organized crystalline to a random, gel-like state, and the triple helix melts and progressively dissociates into the three randomly coiled peptide alpha-chains [38,39]. The resultant effect of collagen fiber denaturation is the

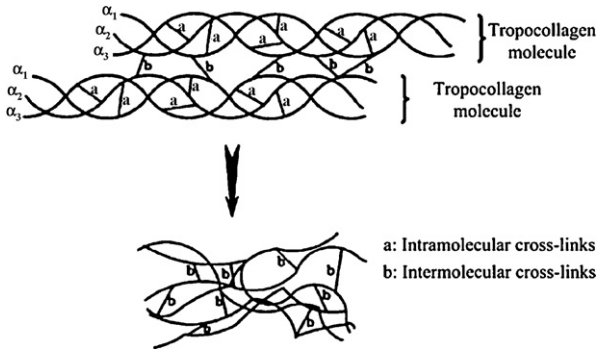

Fig. 5. Schematic of thermal denaturation of collagen molecule [37].

shrinkage of skin [24]. The length of collagen fiber can shrink to one third of its original length under heating above 65 °C [24]. Therefore, significant change in collagen fiber configuration in dermis can be observed after thermal damage. The collagen fibers melt and the blank regions between collagen fibers decreased when the heating temperature increased. However, the cell nucleus kept intact due to their thermal stability [40]. Compared with the control group, the other four sample groups showed a distinct denaturation of collagen fibers after 10 min heating, resulting in the decreased contribution of collagen fibers in bearing mechanical loading.

H&E staining has the resolution at microscale level, which can be applied for identifying thermal damage at collagen fiber level. Longer time (*i.e.*, 10 min) is needed for obtaining comparable thermal effect on the fiber melting (Fig. 4a-e). TEM observation has resolution at nanoscale level. Here we used typical TEM results (60 °C, 30 s) to demonstrate that thermal damage occurs within collagen fibrils (composition of a single collagen fiber) under even shorter thermal treatment. The changes in the cross and longitudinal sections of collagen fibrils before and after exposure to 60 °C for 30 s were depicted in Fig. 6. Before thermal damage, a distinct spacing can be identified between neighboring fibrils (Fig. 6a). The average diameter of the fibrils is estimated as 50 nm. Compared with the control specimens, the thermally damaged samples showed a blurry boundary between collagen fibrils (Fig. 6b) with average fibril diameter of 80 nm which is over 1.5 times larger than that of undamaged fibrils. The transverse striations of collagen fibrils are clearly observed in Fig. 6c. Whereas, such transverse striations became blurry in thermally damaged samples (Fig. 6d). There is a thermally labile domain near the C-terminus of the collagen molecular, from which the denaturation is initiated [41]. The domain is devoid of hydroxyproline, supporting the role of hydrogen bonded water-bridges (linked through hydroxyproline residues) in stabilizing the triple helix. Because the C-terminus is located at the end of collagen molecule (Fig. 7), the transverse striations, spaced approximately 67 nm apart, become vague when the sample is subjected to a gradually elevated temperature.

3.3. Prediction of thermal damage degree

Different metrics based on biological [42], thermal [41] and mechanical [16] features of skin tissue have been proposed to characterize the thermal damage. Here, the Arrhenius burn integration was used to simulate the damage process [25,26]:

$$\Omega = \int_0^t A \ \exp\left(-\frac{E_a}{RT}\right) dt \tag{1}$$

$$Deg(t) = 1 - \exp[-\Omega(t)] \tag{2}$$

where t(s) is the exposure time, T(K) is the heating temperature, Ω is the dimensionless indicator of thermal injury, *Deg* is the degree

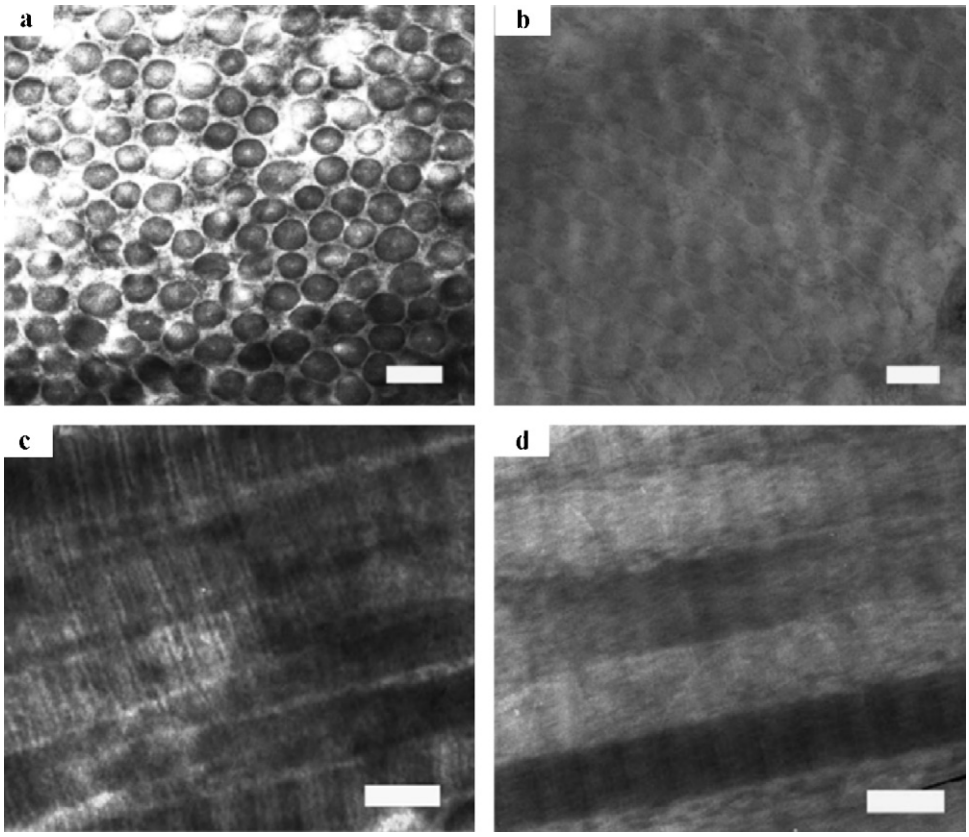

Fig. 6. TEM images of cross sections (a and b) and longitudinal sections (c, d) of collagen fibrils. (a) and (c), control samples exposed to 37 °C; (b) and (d), samples under the heating temperature of 60 °C for 30 s. The boundary and the transverse striations of collagen fibrils were clearly observed in the control samples (a and c). The diameter of collagen fibrils increased and the boundary between the collagen fibrils and the transverse striations were blurry due to thermal denaturation (b and d). Scale bar in (a) and (b): 200 nm. Scale bar in (c) and (d): 100 nm.

of thermal denaturation, $A = 3.1 \times 10^{98}\ s^{-1}$ is a material parameter equivalent to a frequency factor, $E_a = 6.27 \times 10^5$ J/mol is the activation energy, $t_{(h)} = 600$ s is the heating duration and $R = 8.314$ J/mol K is the universal gas constant.

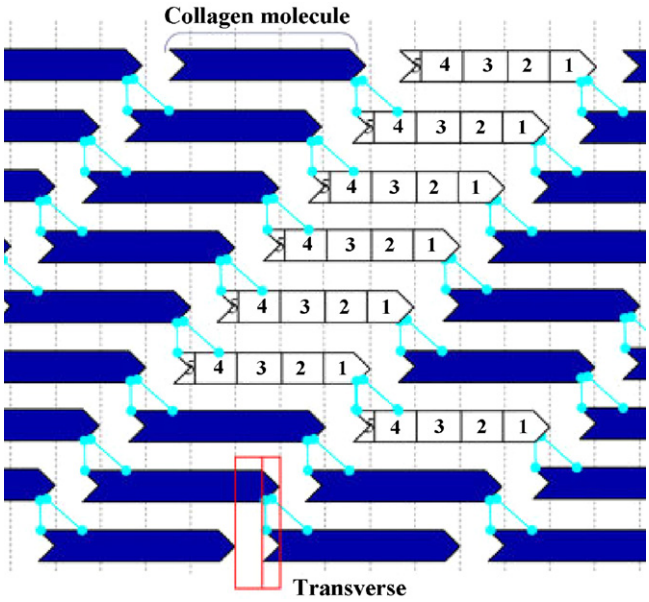

Fig. 7. Schematic of microfibril composed of collagen molecules with gaps and overlaps.

When the specimens were heated in saline, the collagen fibers denature and the area of melted collagen fibers increases with heating temperature (Fig. 4a–e). To quantify this, we measured the area percentage of the melted collagen fibers in the H&E staining photograph using NIH software Image J for characterization of skin thermal damage. The percentage of collagen fiber area at a certain temperature is defined as P_T and a new dimensionless indicator of thermal damage degree $\varphi(T)$ can be written as:

$$\phi(T) = \frac{P_T - P_{37}}{P_{70} - P_{37}} \tag{3}$$

where P_{37} and P_{70} are the mean percentage of collagen fiber area in mounts of H&E staining photographs of samples heated at 37 °C and 70 °C, respectively. The new parameter, $\phi(T)$, was defined as the ratio of increased fiber area (P_T–P_{37}) to the maximum change in fiber area (P_{70}–P_{37}). The sample heated at 37 °C was not denatured, so $\phi(37) = 0$. Five samples were repeated at 70 °C; all the H&E staining images show that the collagen fibers were completely melted (Fig. 4e). The thermal damage reached the upper limit when the sample was heated at 70 °C. Therefore, $\phi(70) = 1$ was defined. The values of P_T in the thermal damage tests at 37 °C, 45 °C, 50 °C, 60 °C and 70 °C were obtained from the H&E staining results. $\phi(T)$ at each individual temperatures was calculated and were shown as means ± standard deviation. *t*-Test was performed to check the variation. In view of the melting in collagen fibers, the severity of thermal damage increased with increasing heating temperature (Fig. 4a–e). Since skin damage due to thermal lesion is an exponential function of temperature, as shown by Eq. (1), a slight increase in heating temperature will significantly influence the predicted value of thermal damage degree. Comparison between the measured and predicted results from Eq. (2) is shown in Fig. 8. The

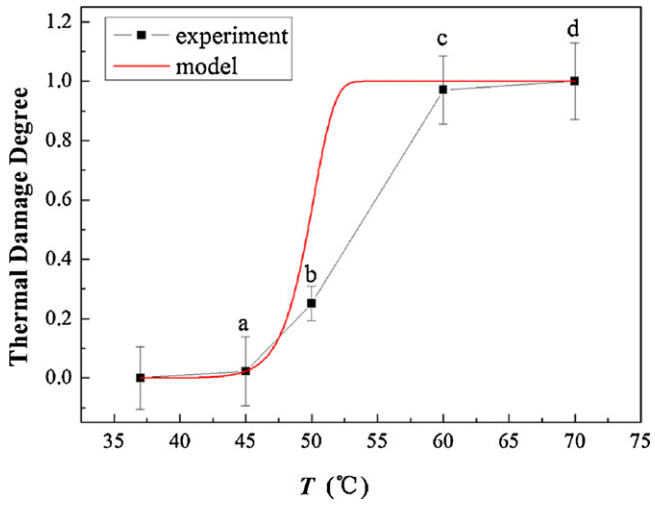

Fig. 8. Comparison between the experimental results and model predictions. P values were estimated using *t*-test. $P > 0.05$ corresponds to experimental data at 37 °C and 45 °C; $P > 0.05$, $P < 0.05$ and $P > 0.05$ correspond to experimental data at 45 °C, 50 °C, 60 °C and 70 °C, respectively.

experimental results correlated well with the predicted results by Arrhenius burn integration in terms of the same variation tendency of thermal damage with heating temperature. These results indicate that the area percentage change can be used as an alternative parameter for quantification of skin thermal damage.

4. Conclusions

In this study, we investigated the effect of thermal damage on the mechanical behavior and microstructure of skin tissue and found that the heating temperature plays an important role in the mechanical behavior and microstructure of the damaged skin tissue. When exposed to a supra-physiological temperature, skin tissue was thermally damaged, accompanied by an increased collagen fibril diameter and a blurry boundary between collagen fibrils. The transverse striations, the main characteristics of microfibril, became less obvious due to the high temperature denaturation. The Young's modulus of skin tissue decreased with increasing heating temperature, which was correlated to the skin microstructure change induced by thermal denaturation of collagen fibers. The thermal damage obtained from experiments agrees well with that predicted by the Arrhenius burn integration. This study aims to explain the macro mechanical behavior of the skin from the angle of its microstructure and to provide insight into the significant role of skin microstructure in the thermomechanical behavior of the skin. Future work will focus on mathematical modeling to better understand the coupling between skin structure and thermomechanical behaviors.

Acknowledgments

This work was supported by the Major International (Regional) Joint Research Program of China (11120101002); National Natural Science Foundation of China (10825210, 31050110125); and the National 111 Project of China (B06024).

Conflict of interest

None declared.

References

[1] Asahina A, Watanabe T, Kishi A, Hattori N, Shirai A, Kagami S, et al. Evaluation of the treatment of port-wine stains with the 595-nm long pulsed dye laser: a large prospective study in adult Japanese patients. J Am Acad Dermatol 2006;54:487–93.
[2] Kono T, Groff WF, Sakurai H, Takeuchi M, Yamaki T, Soejima K, et al. Evaluation of fluence and pulse-duration on purpuric threshold using an extended pulse pulsed-dye laser in the treatment of port wine stains. J Dermatol 2006;33:473–6.
[3] Kauvar ANB, Rosen N, Khrom T. A newly modified 595-nm pulsed dye laser with compression handpiece for the treatment of photodamaged skin. Lasers Surg Med 2006;38:808–13.
[4] Pustovalov V, Jean B. Melanin granule models for the processes of laser-induced thermal damage in pigmented retinal tissues. I. Modeling of laser-induced heating of melanosomes and selective thermal processes in retinal tissues. Bull Math Biol 2007;69:245–63.
[5] Wust P, Hildebrandt B, Sreenivasa G, Rau B, Gellermann J, Riess H, et al. Hyperthermia in combined treatment of cancer. Lancet Oncol 2002;3:487–97.
[6] Yu XF, Li M, Xie MY, Chen LD, Li Y, Wang QQ. Dopant-controlled synthesis of water-soluble hexagonal $nayf_4$ nanorods with efficient upconversion fluorescence for multicolor bioimaging. Nano Res 2010;3:51–60.
[7] Garden JM, Bakus AD, Domankevitz Y. Cutaneous compression for the laser treatment of epidermal pigmented lesions with the 595-nm pulsed dye laser. Dermatol Surg 2008;34:179–83.
[8] Liao HY, Belkoff SM. A failure model for ligaments. J Biomech 1999;32:183–8.
[9] Fratzl P. Cellulose and collagen. From fibres to tissues. Curr Opin Colloid Interface Sci 2003;8:32–9.
[10] Baer E, Hiltner A, Morgan RJ. Biological and synthetic hierarchical composites. Phys Today 1992;45:60–7.
[11] Meyers MA, Chen PY, Lin AYM, Seki Y. Biological materials: structure and mechanical properties. Prog Mater Sci 2008;53:1–206.
[12] Agache PG, Monneur C, Leveque JL, Rigal JD. Mechanical properties and Young's modulus of human skin in vivo. Arch Dermatol Res 1980;269:221–32.
[13] Flory PJ. Role of crystallization in polymers and proteins. Science 1956;124:53–60.
[14] Wright NT, Humphrey JD. Denaturation of collagen via heating: an irreversible rate process. Ann Rev Biomed Eng 2002;4:109–28.
[15] Huang CY, Wang VM, Flatow EL, Mow VC. Temperature-dependent viscoelastic properties of the human supraspinatus tendon. J Biomech 2009;42:546–9.
[16] Chen SS, Humphrey JD. Heat-induced changes in the mechanics of a collagenous tissue: pseudoelastic behavior at 37 °C. J Biomech 1998;31:211–6.
[17] Consigny PM, Teitelbaum GP, Gardiner GA, Kerns WD. Effects of laser thermal angioplasty on arterial contractions and mechanics. Cardiovasc Intervent Radiol 1989;12:83–7.
[18] Kang T, Resar J, Humphrey JD. Heat-induced changes in the mechanical-behavior of passive coronary-arteries. ASME Trans J Biomech Eng 1995;117:86–93.
[19] Kiss MZ, Daniels MJ, Varghese T. Investigation of temperature-dependent viscoelastic properties of thermal lesions in ex vivo animal liver tissue. J Biomech 2009;42:959–66.
[20] Xu F, Lu TJ, Seffen KA. Thermally-induced change in the relaxation behaviour of skin tissue. ASME Trans J Biomech Eng 2009;131:071001.
[21] Lennox FG. Shrinkage of collagen. Biochim Biophys Acta 1949;3:170–87.
[22] Harris JL, Humphrey JD. Kinetics of thermal damage to a collagenous membrane under biaxial isotonic loading. IEEE Trans Biomed Eng 2004;51:371–9.
[23] Chachra D, Gratzer PF, Pereira CA, Lee JM. Effect of applied uniaxial stress on rate and mechanical effects of cross-linking in tissue-derived biomaterials. Biomaterials 1996;17:1865–75.
[24] Arnoczky SP, Aksan A. Thermal modification of connective tissues: basic science considerations and clinical implications. J Am Acad Orthop Surg 2000;8:305–13.
[25] Henriques FC, Moritz AR. Studies of thermal injury. 1. The conduction of heat to and through skin and the temperatures attained therein—a theoretical and an experimental investigation. Am J Pathol 1947;23:531–49.
[26] Moritz AR, Henriques FC. Studies of thermal injury. 2. The relative importance of time and surface temperature in the causation of cutaneous burns. Am J Pathol 1947;23:695–720.
[27] Xu F, Wen T, Seffen KA, Lu TJ. Biothermomechanics of skin tissue. J Mech Phys Solids 2008;56:1852–84.
[28] Xu F, Lu TJ, Seffen KA. Biothermomechanical behavior of skin tissue. Acta Mech Sin 2008;24:1–23.
[29] Daly CH. Biomechanical properties of dermis. J Invest Dermatol 1982;79:S17–20.
[30] Lanir Y. Structural theory for the homogeneous biaxial stress–strain relationships in flat collagenous tissues. J Biomech 1979;12:423–36.
[31] Fratzl P, Misof K, ZizakGert I. Fibrillar structure and mechanical properties of collagen. J Struct Biol 1998;122:119–22.
[32] Melis P, Noorlander ML, van der Horst CMAM, van Noorden CJF. Rapid alignment of collagen fibers in the dermis of undermined and not undermined skin stretched with a skin-stretching device. Plast Reconstr Surg 2002;109:674–80.
[33] Whitton JT, Everall JD. In: Fratzl P, editor. Thickness of epidermis. Collagen fibrillar structure and hierarchies. New York: Springer US; 1973.
[34] Hepworth DG, Steven-fountain A, Bruce DM, Vincent JFV. Affine versus non-affine deformation in soft biological tissues, measured by the reorientation and

stretching of collagen fibres through the thickness of compressed porcine skin. J Biomech 2001;34:341–6.
[35] Hunziker EB, Schenk RK. Cartilage ultrastructure after high-pressure freezing, freeze substitution, and low-temperature embedding.2. Intercellular matrix ultrastructure-preservation of proteoglycans in their native-state. J Cell Biol 1984;98:277–82.
[36] Davidson JM, Zang MC, Zoia O, Giro MG. Regulation of elastin synthesis in pathological states. Mol Biol Pathol Elastic Tissue 1995;192:81–99.
[37] Arnoczky S, Aksan A. Thermal modification of connective tissues: basic science considerations and clinical implications. J Am Acad Orthop Surg 2000;8:305.
[38] Bailey A. Procter memorial lecture. Collagen-nature's framework in the medical, food and leather industries. J Soc Leather Technol Chem 1991;76:111–27.
[39] Kopp J, Bonnet M, Renou J. Effect of collagen crosslinking on collagen-water interactions (a dsc investigation). Matrix 1989;9:443.
[40] Kampinga HH. Thermotolerance in mammalian-cells—protein denaturation and aggregation, and stress proteins. J Cell Sci 1993;104:11–7.
[41] Miles CA. Kinetics of collagen denaturation in mammalian lens capsules studied by differential scanning calorimetry. Int J Biol Macromol 1993;15:265–71.
[42] Bhowmick S, Swanlund DJ, Bischof JC. Supraphysiological thermal injury in dunning at-1 prostate tumor cells. ASME Trans J Biomech Eng 2000;122:51–9.
[43] Kadler KE, Holmes DF, Graham H, Starborg T. Tip-mediated fusion involving unipolar collagen fibrils accounts for rapid fibril elongation, the occurrence of fibrillar branched networks in skin and the paucity of collagen fibril ends in vertebrates. Matrix Biol 2000;19:359–65.